International Journal of Modern Manufacturing Technologies
ISSN 2067–3604, Vol. XIV, No. 1 / 2022
https://doi.org/10.54684/ijmmt.2022.14.1.98

METALLOGRAPHIC EXAMINATION OF SURFACE LAYER AFTER ELECTRICAL DISCHARGE MACHINING

Andrzej Sokołowski[1], Łukasz Łomozik[2], Henryk Bąkowski [3]

[1]Silesian University of Technology, Faculty of Mechanical Engineering, 18A Konarskiego Street, 44-100 Gliwice, Poland
[2]Sm Hydro, 10B Karolinki Street, 40-467 Katowice, Poland
[3]Silesian University of Technology, Faculty of Transport, 8 Krasinskiego Street, 40-019 Katowice, Poland

Corresponding author: Andrzej Sokołowski, andrzej.sokolowski@polsl.pl

Abstract: This paper presents analysis of the influence of selected electrical parameters of hollowing on the state of the surface layer after electrical discharge machining (EDM). Namely, paper focuses on the analysis of the EDM cutting process, in terms of the influence of individual parameters on the number of occurrences and sizes of erosion craters on the machined surface. The basic parameters include electrical pulse discharge time, electrical discharge pause time, voltage, current amplitude and servo voltage. The initial values of the mentioned parameters were selected based on technology tables provided by the machine manufacturer and on the basis of own empirical tests. The tests were carried out according to static determined poliselective experimental plan (Hartley plan). Analysis of the machined surface was carried out using a scanning microscope (SEM) and an optical microscope. Quantitative metallographic analysis was used to determine the stereological features of erosion craters occurring on the surface of the machined material. The results were illustrated by means of three-dimensional graphs. The presented studies show a significant effect of electrical parameters of EDM on the quality of the machined surface, i.e. the number of occurrences and diameter of erosion craters. The research presents an approach based on mathematical modelling of electrical discharge machining. This approach can form the basis for developing methods of modeling technological processes and optimizing their parameters.

Key words: WEDM, surface layer, metallographic examination.

1. INTRODUCTION

The electro-discharge cutting process is well known for its high economic benefits and degree of machining accuracy. Since its introduction in 1969, enormous progress has been made in terms of cutting speed, which is now 4-6 higher and 3-4 times more accurate. Due to the increasing importance of electro-discharge cutting in the industry along with the increasing demands on accuracy and economy of technological processes, there is a need for precise research over the impact exerted by the electro-discharge machining on the quality and effectiveness of the cutting.

The authors of most works on this topic, focus on determining the influence of individual electrical and hydromechanical parameters on the quality of the machined surface, geometric accuracy of the cut parts, and cutting performance. Researchers indicate that the most significant factors in terms of influence on the quality and performance of WEDM cutting are the electrical parameters, especially the duration of the electrical pulse, voltage the electrical current [1,2]. These parameters determine the amount of energy delivered to the erosion gap, which directly affects the size and stability of the plasma channel, which in turn determines the geometric dimensions of the cut workpiece, the structure of the machined surface and affects the stability and speed of machining. According to research (e.g. ([3]), the higher the duration of the electrical pulse, the higher the material removal rate and the lower the quality of the cut surface. Researchers (e.g. [4]) indicate that the electrical voltage is the most significant parameter in terms of affecting the quality of the machined surface (the higher the voltage value, the lower the surface quality), and the intensity of the electrical current is important in controlling the machining speed and geometric accuracy of the cut parts (higher intensity speeds up machining but contributes to shape errors). The results of other studies (e.g. [6,7]) indicate that the speed of wire feeding into the workspace is also important in stabilizing machining - the lower the speed, the higher the probability of wire breakage which forces the machining to slow down and the poorer the quality of the machined surface (by lower uniformity of electrode-material contact) [10]. On the other hand, high wire tension leads to more straightness in the wire, which helps to stabilize the electrical voltage between the two electrodes and create more heat flux, resulting in increased erosion

of the material at the corners and thus dimensional errors (especially corner errors) [9].
This paper focuses on the analysis of the WEDM cutting process, in terms of the influence of individual parameters on the number of occurrences and sizes of erosion craters on the machined surface.

2. MATERIALS AND METHODS

The research was conducted according to Hartley's poliselective experimental plan. According to the plan, the input parameters of the processing were set at three levels - minimum, average, and maximum. The different combinations of parameter levels were implemented according to the experiment plan matrix (Hatley matrix)[5].
The use of a three-level plan allowed us to obtain mathematical models of the studied process in the form of a second-order polynomial (1) [5]:

$$y = b_0 + \sum b_k x_k + \sum b_{kk} x_k^2 + \sum b_{kj} x_k x_j, \quad (1)$$

where**:**
y **-** explained variable
b_k - regression coefficients
x_k - input variables

2.1 Materials and equipment used in the tests

The tests were carried out on chromium-nickel-molybdenum alloy steel 40CrMnNiMo8-6-4 (Table 1) which selected mechanical properties are listed in Table 2. The material was delivered as 280x150x10 plates.

Table 1. Chemical composition of the steel used in the tests [%][13]

C	Si	Mn	Cr	Ni	Mo	S
0.37	0.3	1.4	2.0	1.0	0.2	<0.01

Table 2. Selected mechanical properties of alloyed steel [13]

Trade name of steel	Density [g/cm3]	Hardness [HB]	Tensile strength; Rm, [MPa]	Yield point; Re, [MPa]
IMPAX	7.8	330	1020	900

The cut samples were rectangles with dimensions of 30x15x10 mm (Figure 1). Each specimen contained approximately six sample surfaces cut using different parameters. The considered parameters and ranges of their values are depicted in the consecutive sections of the paper.
Experimental tests were carried out on a Joemars AWT5S WEDM electrical discharge machine. The working electrode was CuZn37 brass wire of 0.25 mm diameter and 900 N/mm^2 strength. The electric medium was distilled and deionized water with a resistance of R = 5·10^4 Ωcm.

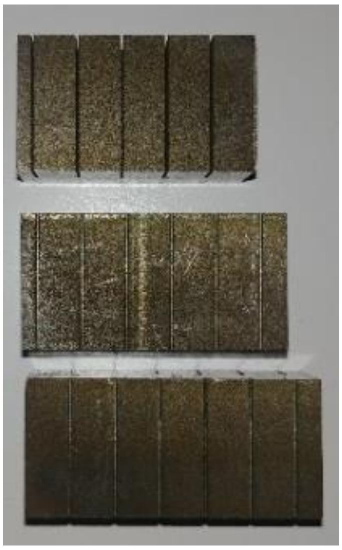

Fig. 1. Cut samples

2.2 Measurement methods

Optical analysis of the machined surfaces was performed using a NEXIV VMA Auto Measure microscope with a 3.5x zoom and automatic measuring of 3D components function, and a scanning electron microscope. The image thresholding technique was used to identify and estimate the dimensions of erosion craters in Metilo software. The dimensions of the craters were defined as shown in Figure 2. The roughness of cut parts was measured on the SRT-6210 needle profile meter.

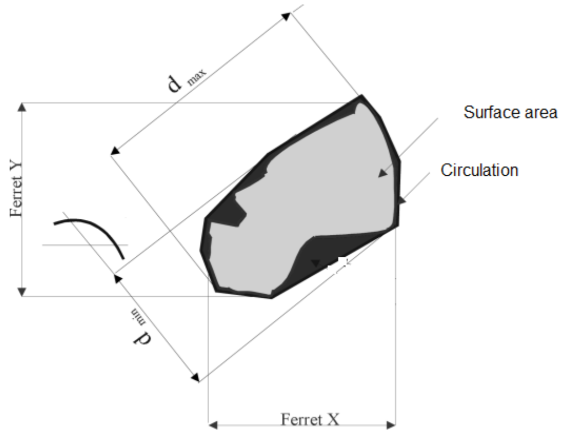

Fig. 2. Dimensions of craters

2.3 Selection of the parameters under consideration

The basis for determining the appropriate input parameters for the experimental tests was to determine their actual values and the adjustable variability ranges for the adopted type of planned experiment. Input factors X_1, X_2, X_3 and X_4 (see equation (1)) are respectively the wire feed rate WF, the electric pulse time ON, pause time between pulses OFF and electrical voltage OV.

Using the recommended values of the machine manufacturer's parameters [8] and the literature analysis, tests were carried out to check the maximum, central and minimum levels of the considered parameters for machining stability (Table 3).

The number of occurrences of erosion craters Nc, the maximum diameter of craters Dc and additionally the surface roughness parameters Ra, Rz, Rq, and Rt were taken as evaluation of machining parameters (Table 4).

Table 3. Selection of parameters for testing

No.	Parameter	Variable	Minimum value	Average value	Maximum value	Unit
1	OV	X_1	80	90	100	V
2	ON	X_2	10	11	12	µs
3	OFF	X_3	9	10	11	µs
4	WF	X_4	4	7	10	mm/min

Table 4. Selection of output quantities

No.	Variable	Measurement	Unit
1	Ra, Rz, Rq, Rt	Surface roughness parameters	µm
2	D_c	Maximum diameter of erosion craters	µm
3	N_c	Number of occurrences of erosion craters	

3. RESULTS AND DISCUSSION

After technological, metrological and statistical tests, the obtained results are presented in Table 5.

Table 5. A list of test results

Test No	Controlled factors on a real scale				Measurement results					
No	OV [V]	ON [µs]	OFF [µs]	WF [mm/min]	Ra [µm]	Rz [µm]	Rq [µm]	Rt [µm]	D_c [µm]	N_c
1	100	12	11	10	12.02	33.98	12.90	34.32	326.40	2787.84
2	100	12	9	4	12.29	34.77	13.25	35.11	142.30	292.23
3	100	10	11	4	11.22	31.74	12.14	32.05	128.10	584.85
4	100	10	9	10	11.95	33.81	12.71	34.14	269.83	2855.20
5	80	12	11	4	12.41	35.09	13.42	35.44	198.55	2613.45
6	80	12	9	10	12.45	35.29	13.17	35.10	176.00	4501.20
7	80	10	11	10	11.90	33.66	12.69	34.00	144.80	1379.00
8	80	10	9	4	11.80	33.37	12.61	33.70	122.55	1624.50
9	100	11	10	4	12.43	35.17	13.41	35.51	113.14	2344.05
10	80	11	10	4	11.97	33.86	12.87	34.20	85.47	4219.95
11	90	12	10	4	11.86	33.54	12.84	33.87	346.50	3931.40
12	90	10	10	4	11.84	33.49	12.98	33.83	98.61	5061.45
13	90	11	11	4	13.39	37.88	14.32	38.25	421.47	3596.67
14	90	11	9	4	11.97	33.86	13.05	34.20	102.60	4443.15
15	90	11	10	10	13.53	38.17	14.37	38.39	173.81	3691.08
16	90	11	10	4	12.67	35.84	13.61	36.19	185.25	4332.00
17	90	11	10	4	12.55	35.50	13.56	35.85	197.40	5457.90

3.1 Statistical model analysis

The research was carried out with the assumed level of significance α = 0.05. In the tables below (Table 6, Table 7), the mean values of two actual measurements of the examined dependent variable based on the measurement results from Table 5, the corresponding values obtained from the designated regression function and the square differences of these values, determining the error of the applied mathematical model are presented.

Table 6. Experimental results of the number of erosion crater occurrences N_c and regression function results $\widehat{N}_c$

No	N_c	$\widehat{N}_c$	Error [%]
1	2787.84	3567.5234	27.97
2	292.23	223.8504	23.40
3	584.85	327.9874	43.92
4	2855.2	2414.9384	15.42
5	2613.45	2329.5984	10.86
6	4501.2	3651.3494	18.88
7	1379.0	1396.9764	1.30
8	1624.5	3535.5234	117.64
9	2344.045	2853.639	21.74
10	4219.95	3948.426	6.43
11	3931.4	5006.9027	27.36
12	5061.45	4482.6787	11.43
13	3596.67	3863.498	7.42
14	4443.15	4414.392	0.65
15	3691.075	4707.301	27.53
16	4332.0	3553.844	17.96
17	5457.9	4744.7907	13.07

Table 7. Experimental results of the maximum diameter of erosion craters D_c and regression function results $\widehat{D}_c$

No	D_c	$\widehat{D}_c$	Error [%]
1	326.4	422.2477	29.37
2	142.295	115.1542	19.07
3	128.1	111.1892	13.20
4	269.825	255.8647	5.17
5	198.55	308.9527	55.60
6	176.0	127.4932	27.56
7	144.795	123.5282	14.69
8	122.55	142.5697	16.34
9	113.135	125.3399	10.79
10	85.47	74.8619	12.41
11	346.5	265.9379	23.25
12	98.605	180.7639	83.32
13	421.47	303.4379	28.00
14	102.6	222.2289	116.60
15	173.81	224.1136	28.94
16	185.25	161.2966	12.93
17	197.4	192.7051	2.38

Based on the above-mentioned tables, the scatter plots (Figure 3, Figure 4) of real data, i.e. measurement results, and the dependent variable resulting from the regression equation was determined.

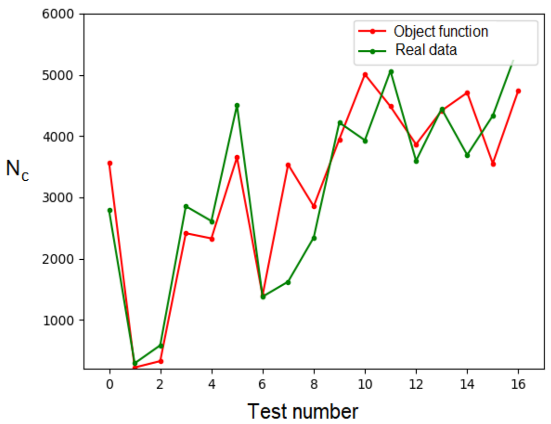

Fig. 3 Scatter plot for the explained variable - number of occurrences of erosion craters

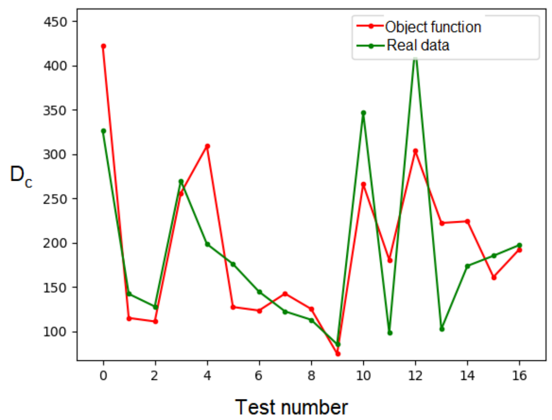

Fig. 4 Scatter plot for the explained variable - maximum diameter of erosion craters

$$N_c = 390.46 \cdot ON \cdot OFF + 556.92 \cdot ON - 605.85 \cdot OFF^2 + +19.36 \cdot OFF + 3206.61 \quad (2)$$

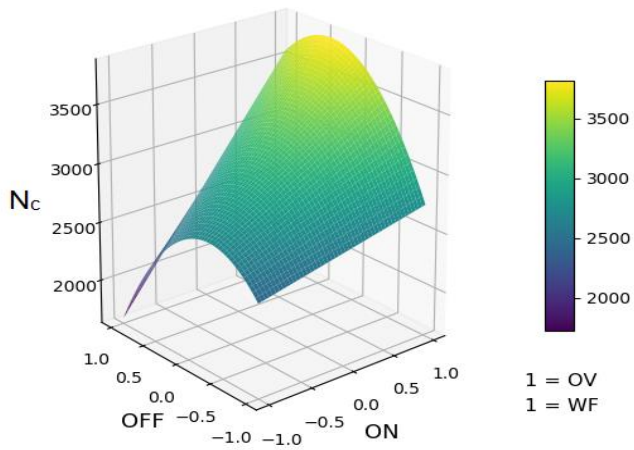

Fig. 5 Influence of OFF pulse interval time and ON pulse time on the number of erosion crater occurrences based on equation (2)

$$N_c = -1343.76 \cdot OV^2 - 547.39 \cdot OV + 262.11 \cdot ON + 4744.79 \quad (3)$$

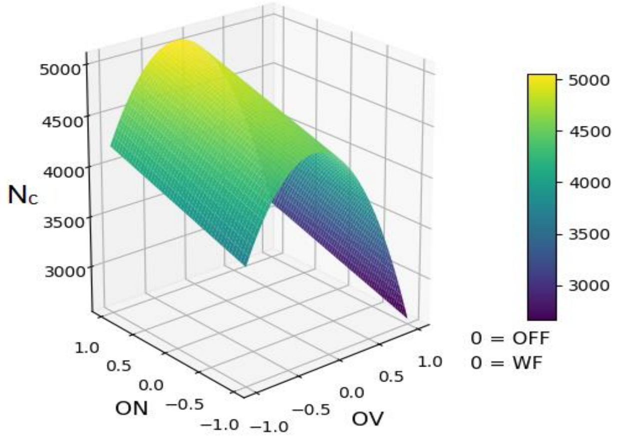

Fig. 6 Influence of ON pulse time and electrical voltage OV on the number of erosion crater occurrences based on equation (3)

$$D_c = 30.65 \cdot ON^2 + 42.59 \cdot ON - 9.36 \cdot WF + 74.87 \quad (4)$$

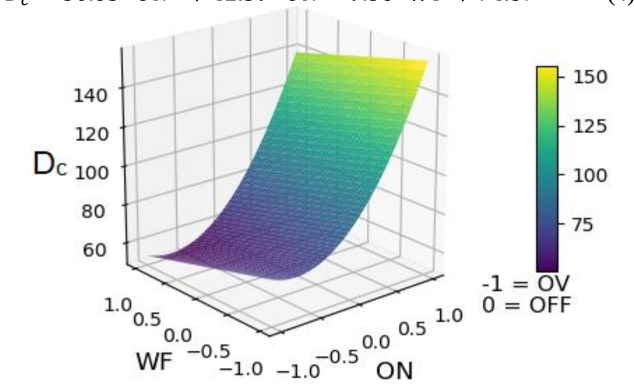

Fig. 7 Influence of ON pulse time and WF wire winding speed on the maximum diameter of erosion craters based on equation (4)

3.2 Analysis of test results

Application of the experimental data modelling allowed to determine the main trends in the process of erosion crater formation. Based on the tests carried out, three-dimensional graphs determined from the second-degree polynomial function (equation 2-4) were developed (Figures 5-7).

The process of crater formation on the surface of the anode (workpiece) is the result of electron emission from the cathode [11], which causes ionization of the dielectric and formation of a plasma channel. The electric current flowing through the channel causes local melting, boiling and evaporation of the workpiece material. The relationships shown in Figures 5 and 6 show that with increasing pulse time there is an increase in the frequency of occurrence and diameter of erosion craters. This effect indicates significant changes in the heat flux density inside the plasma channel, depending on the pulse time. Figure 7 shows the relationship between the electrical discharge voltage, pulse time, and the occurrence of erosion craters. It can be seen that, as mentioned earlier, an increase in ON causes an increase in the number of craters. An increase in voltage, on the other hand, causes a significant decrease in the number of craters. This is most probably due to the fact that high electric voltage stabilizes the plasma channel, slowing down the cutting process and thus obtaining a more uniform surface [12]. The WF parameter, as can be seen among others from Figure 7, has a negligible effect on the formation and shape of erosion craters.

To confirm the presence of craters on the optically tested surfaces, additional surface roughness tests were performed. Simplified plots of the surface topography were prepared based on the tests (Figure 8). These tests confirm the identified craters and indicate the stochastic nature of their distribution on the sample surface.

The following SEM microscope images (Figure 9) show examples of erosion craters. Their dimensions agree with the estimates resulting from surface roughness measurements and threshold analysis of the optical microscope image.

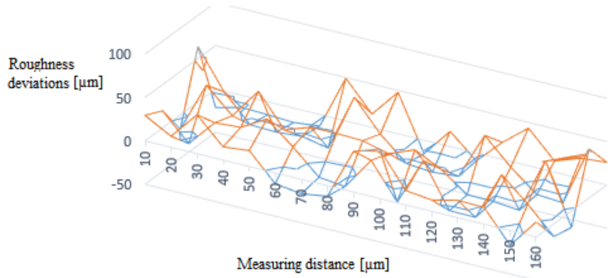

Fig. 8 Simplified topography of the specimen surface

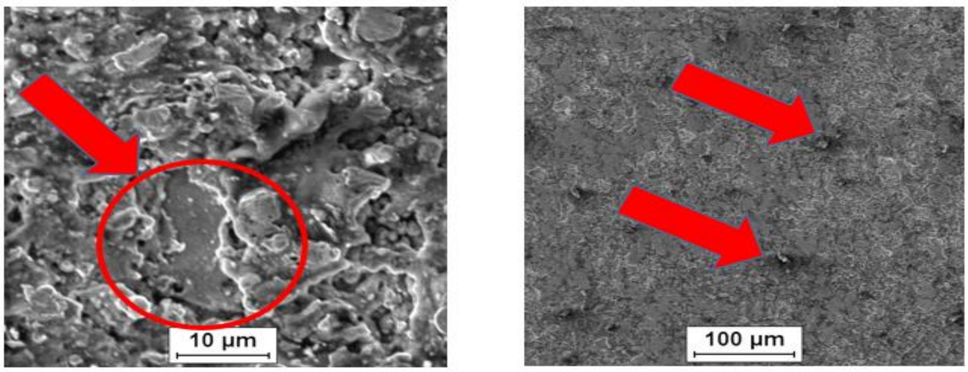

Fig. 9. Scanning microscope SEM images with erosion craters highlighted

4. CONCLUSIONS

The study shows that parameters such as ON pulse time and electrical voltage OV have a significant effect on the frequency and size of erosion craters. The longer the ON pulse time, the more craters and the larger their diameter. On the other hand, the OV parameter inversely affects the frequency of craters. The above observations show that the optimal parameter levels in terms of the obtained surface quality are minimum ON time and maximum OV voltage. However, such a setting has a negative effect on the machining speed, which can be partially compensated in economic terms by reducing the speed of scrolling of the working electrode, since the studies show that the WF parameter in the studied range does not affect the analysed output factors.
The study also proves the possibility of modelling the EDM process using mathematical models, which can form the basis for building more comprehensive models and programs to optimize the parameters of the EDM cutting process, and potentially other technological processes depending on the given optimization criteria.

5. REFERENCES

1. Bose, S., Nandi, T. (2021). *Measurement of performance parameters and improvement in optimized solution of wedm on a novel titanium hybrid composite*, Measurement, 171.
2. Chaudhari, R., Vora, J., Prabu, S., Palani, I., Patel, V. K., Parikh, D. M. (2019), *Pareto optimization of WEDM process parameters for machining a NiTi shape memory alloy using a combined approach of RSM and heat transfer search algorithm*, Advances in Manufacturing, 9.
3. Ishfaq, K., Anwar, S., Ali, M., Raza, M., Farooq, M., Ahmad, S., Pruncu, C., Saleh, M., Salah, B. (2020), *Optimization of WEDM for precise machining of novel developed Al6061-7.5% SiC squeeze casted composite*, The International Journal of Advanced Manufacturing Technology, 111, 1-19.
4. Kavimani, V., Prakash, K., Thankachan, T., Nagaraja, S., Jeevanantham, A., Jhon, J. P. (2019), *WEDM Parameter Optimization for Silicon/Magneisum Composite Using Taguchi Based GRA Coupled PCA*, Silicon, 12, 1161-1175.
5. Korzyński M., (2017), Metodyka eksperymentu, 195-209, Polish Scientific Publishers PWN, Warsaw.
6. Łomozik Ł., Bąkowski H., Sokołowski, A., (2020), *Influence of selected hydromechanical parameters of WEDM machine on quality and cutting performance*, Int. J. Mod. Manuf. Technol., 12 (3), 78-83.
7. Meena, K. L., Manna A., Banwait S. S., Jaswanti., (2013), *Effect of wire feed rate and wire tension during machining of pr-al-sic-mmc by wedm*. European Journal of Engineering and Technology, 1 (1).
8. Nakamachidai, Tsuzuki-ku, (2005), Instrukcja Obsługi. *Układ sterowania wycinarką drutową LN1W*, 15-17, Sodick Corporation, Yokohama.
9. Pramanick, A., Mandal, S., Dey, P., Das, P. K., (2021), *WEDM process optimization of sintered structural ceramic sample by using fuzzy-MPCI technique*, Materials Today: Proceedings, 41, 925-93.
10. Rozenek M, Dąbrowski, L., (2011), *Aspekty ekonomiczne i dokładnościowe wycinania elektroerozyjnego*. Archives of Mechanical Technology and Materials, 31 (2), 87-95.
11. Scott D., Boyina S., (1990), *Analysis and optimization of parameter combinations in wire electrical discharge machining*. International Journal of Production Research, 29(11), 2189-2207.
12. Świercz R., Oniszczuk-Świercz D., (2014), *Wpływ parametrów obróbki elektroerozyjnej na właściwości użytkowe stali o wysokiej przewodności cieplnej*. 1, 29-33.
13. *Uddeholm impax supreme*. Available from: https://www.uddeholm.com/app/uploads/sites/40/2017/11/impax_supreme-eng_p_1109_e7.pdf, Accesed: 08/11/2018.

6. ACKNOWLEDGEMENTS

This research was co-financed by the Ministry of Education and Science of Poland under grant No RJO15/SDW/004_05

Received: February 16, 2022 / Accepted: June 15, 2022 / Paper available online: June 20, 2022